Green Chemistry

PAPER

View Article Online
View Journal | View Issue

Cite this: *Green Chem.*, 2026, **28**, 5701

A combined microwave/continuous flow approach for the iodination of anilines and consecutive Mizoroki–Heck cross-coupling

Matteo Bartalucci,†[a] Filippo Bocerani,†[a] Francesco Ferlin,[a] Luciano Lattuada,[b] Fulvio Uggeri[b] and Luigi Vaccaro*[a]

Received 17th December 2025,
Accepted 24th February 2026

DOI: 10.1039/d5gc06815k

rsc.li/greenchem

Within this work, we report a modular, microwave-assisted continuous-flow approach for the selective iodination of unprotected anilines, achieving control of regioselectivity, over-halogenation, and the need for a protecting group. Microwaves (MW) irradiation enables rapid and localised energy transfer to accelerate kinetics and suppress by-product formation, while the use of a recoverable reaction medium as acetonitrile–water azeotrope (ACN/H_2Oaz) led to substantial improvements in both reaction mass efficiency (RME) and *E*-factor. Moreover, it has been demonstrated that the protocol can be telescoped by combining MW/flow iodination and the representative Mizoroki–Heck reaction in continuous flow. The protocol eliminates the need for intermediate isolation and solvent switching. This integrated process delivers functionalized products rapidly, with high selectivity and reduced waste compared to conventional protocols.

Green foundation

1. Our methodology offers a rapid, selective, and sustainable strategy to achieve the selective iodination of anilines ready for the subsequent cross-coupling reactions in batch and continuous-flow conditions.
2. Careful selection of conditions and reagents resulted in a very low *E*-factor and high reaction mass efficiency. Metrics were calculated for all compounds synthesized using our telescoped continuous-flow methodology, including API key intermediates.
3. In future work, the presented strategy could also be evaluated by considering the toxicity, safety, and LCA data of the different materials used for the procedures available. It could be expanded by integrating other types of cross-coupling or C–H activation processes.

Introduction

A modular approach to flow technologies has revolutionized process chemistry practice concerning the synthesis of functionalized compounds, especially in pharmaceuticals, agrochemicals, and materials science.[1,2] It is of great interest to combine different reactivities and realize multistep synthetic sequences in flow that combine selective reactions conditions in an integrated, scalable, and reproducible manner.[3,4] One example of our interest is the synthesis of functionalized aryl intermediates. This represents a bottleneck in many production sequences,[5] where site selectivity and functional group tolerance are required.[6]

Aromatic electrophilic reactions require different thermal and kinetic conditions, as well as chemical compatibility.[7–10] In particular, halogenation of aromatics is a challenging process that requires great care to be adapted to modular reactors because it involves short-lived active species, potentially reactive by-products, and solvent sensitivity.[11] The precise control of regioselectivity in activated substrates, such as anilines, is even more problematic.[12] Usually, temporary amino group protection is employed to overcome these difficulties, often through acyl or carbamate derivatives (*e.g.*, Boc, Acyl, Tosyl), followed by deprotection at the end of the sequence.

The procedures, even if highly efficient, significantly increase the length of the synthetic sequence, reagent consumption, and waste production, and also impose limits on the modularity and scalability of the entire process.

Among the most useful halogenated compounds, iodinated anilines occupy a prominent position due to their use as key intermediates in C–C, C–N, and C–O bond formation processes, typically *via* cross-coupling or C–H activation

[a]*Laboratory of Green S.O.C. – Dipartimento di Chimica, Biologia e Biotecnologie, Università degli Studi di Perugia, Via Elce di Sotto 8, 06123 Perugia, Italy. E-mail: luigi.vaccaro@unipg.it; https://greensoc.chm.unipg.it*
[b]*Bracco Imaging SpA, via Egidio Folli 50, 20134 Milano, Italy*
†These authors have contributed equally to this work.

reactions.[13–15] They are also important building blocks for the synthesis of industrially produced iodinated contrast agents.[16]

Due to the high reactivity of the C–I bond, iodo-derivatives are generally preferred over less-reactive chlorides and bromides if the complexity of the target increases. This is true in terms of reactivity and environmental impact.[17]

However, direct introduction of iodine onto unprotected anilines presents considerable practical and synthetic difficulties, thereby representing a challenge for synthetic organic chemistry.[18,19]

In fact, aromatic amines are highly susceptible to electrophilic substitution reactions, which can lead to over-halogenation, uncontrolled regioselectivity, and by-product formation, consequently generating waste materials from purification steps. Additionally, traditional conditions for iodination, based on molecular iodine in the presence of oxidants (most commonly a combination of an acid with a peroxyacid or a peroxide), are often poorly tolerated by sensitive functional groups.[19–21] Therefore, the use of protecting groups is required; however, the direct introduction of iodine, avoiding unnecessary steps, is highly desirable. This necessitates not only a finely tuned design of the reactive conditions, but also active control of energy transfer and the formation of active species.

We directed our attention to the use of microwave (MW) irradiation because it represents an effective tool to control energy transfer during the formation of highly reactive intermediates, such as I^+.[22,23]

MW irradiation is effective in accelerating organic reactions through rapid, selective, and localised energy transfer.[23–25]

In this context, it is noteworthy that the development of a MW-assisted, selective iodination process for unprotected anilines remains underexplored.[26,27]

This study exploits the effect of MW irradiation to generate *in situ* an active iodine species (presumably I^+ or I_3 oxidised) from I_2 and the desired oxidant, thereby enhancing reaction kinetics and reducing by-product formation. This approach improves synthetic efficiency and process sustainability because it reduces overall energy consumption compared with direct heating.[28]

The development of processes that feature high reaction mass efficiency (RME) and intrinsically low waste production is of utmost importance in modern chemical synthesis.[29–36] Many strategies have been developed to attain this goal, and one of the most effective strategies is the use of recoverable reaction media. In fact, solvents typically constitute ~80% of the mass of waste.[37–40] The use of recoverable azeotropes, in this context, is a valid choice because it combines the solvent properties of aqueous/organic mixtures with the additional advantage of being recoverable by distillation at a temperature lower than that of the individual components (minimum azeotrope). Additionally, no iodination processes (nor halogenation in general) performed in azeotropic mixtures have been reported to date.

We aimed to define an MW-assisted selective iodination process for various substituted anilines in a recoverable azeotropic mixture of acetonitrile and water. The efficiency of the process, including the solvent recovery and reuse, was quantified by measuring RME and the *E*-factor.

We also defined a continuous flow methodology that, in combination with MW irradiation, allowed an exceptionally fast and selective process.

Iodinated aromatics are useful for several processes to prepare target materials (*e.g.*, cross-coupling reactions and all the related transformations). Therefore, the flow iodination process was integrated with the widely representative palladium-catalysed Mizoroki–Heck cross-coupling process. This strategy eliminated the need for intermediate isolation or solvent switching, while providing an excellent opportunity for synthesising intermediates of interest in shorter times and with reduced generation of waste.

Results and discussion

We began our investigation by optimising the iodination protocol in batch using MW irradiation as a heating source. 2,6-Diisopropylaniline (**1a**) was used as a model aniline substrate to initially focus only on the chemical efficiency and consider the regioselectivity of the process at a later stage.

The selected aniline (**1a**) was dissolved in the indicated medium, along with the iodination source, hydrogen peroxide, and occasionally an acidic additive to enhance the oxidative nature of the reaction environment. The reaction mixture was allowed to react under closed vessel conditions, and the results are reported in Table 1.

Table 1 Iodination reaction optimisation parameters on 2,6-diisopropylaniline (**1a**)

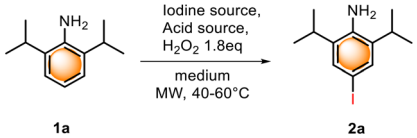

1a **2a**

Entry	Iodine source (eq.)	Acid (eq.)	*W*	Medium	*T* (°C)	Time (s)	*C*[a] (%)
1	NaI (1)	AcOH (8.7)	50	2Me-THF	40	14	80
2	NaI (1)	AcOH (8.7)	20	2Me-THF	60	25	91
3	NaI (1)	PTSA (8.7)	20	2Me-THF	60	80	97
4	NaI (1)	No acid	20	2Me-THF	60	60	—
5	NaI (1)	PTSA (1.2)	20	2Me-THF	60	50	77
6	NaI (1)	PTSA (1)	20	2Me-THF	60	45	94
7	NaI (1)	PS-PTSA (1)	20	ACN/H_2Oaz	48	300	90
8	NaI (1)	PTSA (1)	20	ACN/H_2Oaz	60	50	95
9	I_2 (0.7)	No acid	20	ACN/H_2Oaz	60	65	99
10	I_2 (0.5)	No acid	20	ACN/H_2Oaz	60	65	99
11	I_2 (0.5)	No acid	20	GVL/H_2O[b]	60	70	89
12	I_2 (0.5)	No acid	20	CPME/H_2Oaz	60	65	91

[a] Reaction conditions: 2,6-diisopropylaniline (**1a**) (1 mmol), H_2O_2 (1.8 eq.), iodine source, acid source, medium (1.2 mL). *C* = conversion to **2a**, determined by GLC, and the remaining material was starting **1a**. [b] GVL/H_2O (9 : 1).

In this initial optimisation process, two iodinating agents were tested: sodium iodide (NaI) and molecular iodine (I_2). It became evident that the use of NaI depended on strong acid additives to achieve sufficient efficiency. I_2 did not require such strong oxidative conditions and reacted smoothly without any external acid additive. Both NaI and I_2 enabled complete iodine atom economy (a stoichiometric amount of I equivalents); however, I_2 proved to be a better choice due to the milder reaction conditions required. Moreover, the use of NaI could be less advantageous in terms of atom economy due to the inevitable loss of sodium atoms. Therefore, molecular iodine ensured complete conversion of the starting aniline (**1a**) within ~1 min without the addition of an acid.

During this initial optimisation screening, we also investigated various "green" solvents and mixtures known for their interesting recovery capabilities.[29,31,38,39] 2-MeTHF, CPME/H_2O and ACN/H_2O azeotropic mixtures, as well as a GVL/H_2O (1 : 1) mixture, were tested. Under identical experimental conditions (Table 1, entries 6 and 8), 2-MeTHF and the ACN/H_2O azeotrope allowed for approximately the same conversion. However, the aqueous mixture showed increased solubility of all reagents, making it our preferred choice as the reaction medium. Additionally, the CPME/H_2O azeotrope and the GVL/H_2O (1 : 1) mixture were tested in the optimisation process. However, despite achieving very high conversions, they remained lower than those obtained with the ACN/H_2O azeotrope (Table 1, entries 10–12). By setting the MW irradiation power to 20 W and the temperature limit at 60 °C, we achieved an average reaction time of 60 s across all experiments, obtaining complete conversion using a stoichiometric amount of I_2 in the ACN/H_2O azeotrope mixture. With these optimised reaction conditions, we defined the continuous flow conditions (combining MW irradiation and flow chemistry).

Iodination optimisation in continuous flow with MW irradiation as the heating source

A 600 cm PTFE tube with an internal diameter of 1/16″ equipped with an appropriate back pressure regulator (BPR) was coiled and placed inside an MW oven with an open vessel attachment (see the SI for further details). A mixture of 2,6-diisopropylaniline (**1a**), H_2O_2, and I_2 in ACN : H_2O az (azeotrope) was passed through the reactor under MW irradiation, and the results are listed in Table 2.

As a first attempt, we used the same conditions optimised for the batch protocol, but the overall conversion was only slightly above 60%. Decreasing the flow rate under these conditions did not affect the conversion to product **2a** (Table 2, entries 1–3).

Increasing the temperature while simultaneously increasing the MW power (and consequently adjusting the BPR to maintain a constant pressure throughout the system) could lead to improvements in yields (Table 2, entries 4–11). Complete conversion was achieved under the following conditions: **1a** (1 mmol), I_2 (0.5 eq.), H_2O_2 (1.8 eq.), 300 W, 120 °C, with a flow rate of 1 mL min^{-1} (Table 2, entry 11). These reaction conditions enabled a quantitative conversion of 1 mmol of the starting aniline (**1a**) into the desired product (**2a**) with a productivity of 24 mmol h^{-1}. Notably, compared with the batch process, these flow conditions were more effective, especially from a scalability perspective.

Table 2 Optimisation of iodination reaction conditions in continuous flow with MW irradiation as the heating source

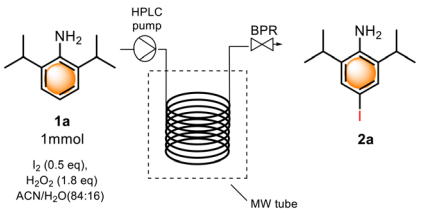

Entry	W	T (°C)	BPR (psi)	Flow rate (mL min^{-1})	Residence time (min)	C^a (%)
1	20	60	45	4	3	62
2	20	60	45	3	3.2	60
3	20	60	45	1	3.3	64
4	30	90	75	2	4.2	71
5	30	90	75	1	4.5	77
6	60	70	75	1	3	68
7	120	85	75	1	2.5	76
8	150	90	75	1	3.1	71
9	200	95	75	1	3.1	79
10	250	100	100	1	2.5	91
11	300	120	100	1	2.5	98 (95)

[a] Reaction conditions: a 0.8 M solution of 2,6-diisopropylaniline (**1a**, 1 mmol), I_2 (0.5 eq.), H_2O_2 (1.8 eq.) in ACN/H_2O (84 : 16) was flowed through the reactor under MW irradiation. Fixed power program. C = conversion to **2a** determined by GLC, and the remaining material is unreacted **1a**. Yield is given in parentheses.

As planned, the work-up and purification to obtain pure product **2a** were simplified using a recoverable azeotropic mixture as the medium. From the crude reaction mixture, ACN/H_2O az was distilled and recovered in about ~92%. Subsequently, the dried mixture of isomers was purified to confirm their structure and ratios.

The optimised conditions were extended to several substrates (Scheme 1), yielding iodinated products with good-to-excellent yields. Among the tested substrates, the tolerability of halo-, nitro-, cyano-, and hydroxy-substitution was evaluated, allowing for further orthogonal functionalization. For all the substrates tested, the *para*-position was consistently preferred if free of substitution.

In cases where the *para*-position was occupied, monohalogenation was the major isomer obtained in all instances, except for product **4a**. Interestingly, this product is itself an approved API (iodoquinol) used for amoebiasis.[41]

Interestingly, the Hammett plot (see SI) for the iodination substrate scope (Scheme 1) described above revealed a weak correlation. This indicated that, under optimized conditions for MW irradiation, electronic effects were far less important for explaining the high regioselectivity observed. Further mechanistic insight, using kinetic or competitive experiments (which is outside the scope of the present work), is needed to understand this behaviour.

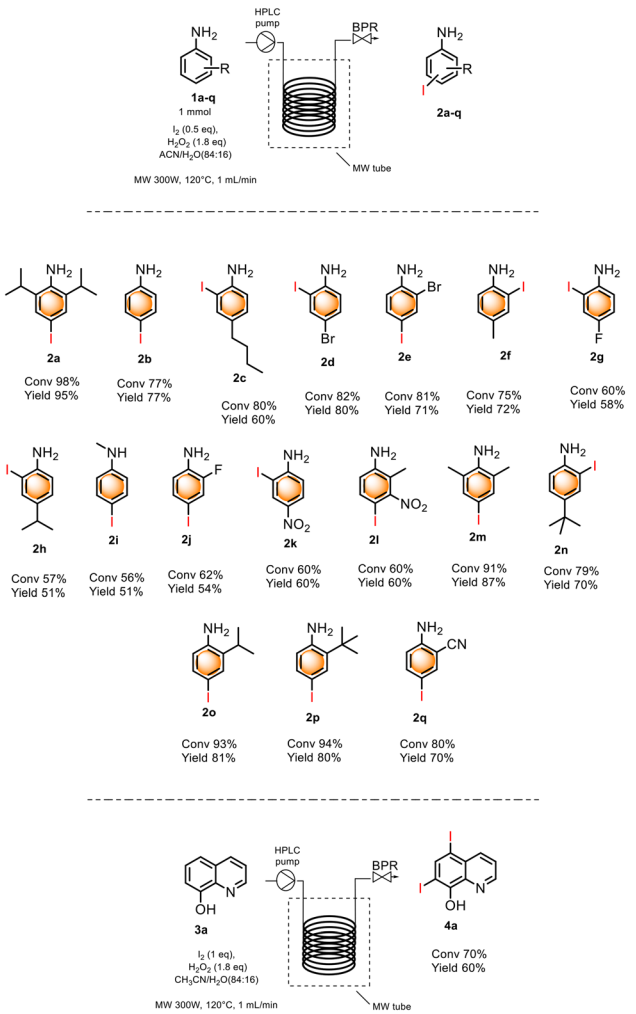

Scheme 1 Substrate scope for continuous flow (under MW irradiation) in the iodination reaction of different substituted anilines. Reaction conditions: aniline (1 mmol), I_2 (0.5 eq.), H_2O_2 (1.8 eq.), ACN/H_2O (84 : 16). 1 eq. of iodine was used to synthesize compounds **2k** and **4a**. Fixed power program. Yields of isolated pure products.

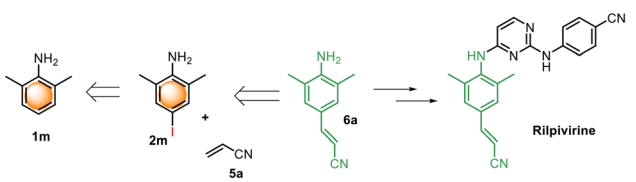

Scheme 2 Intermediate **6a** retrosynthetic scheme.

Within the developed flow procedure, we obtained compound **2m** from 2,6-dimethylaniline (**1m**), which serves as a useful substrate that can be further utilized for the synthesis of the approved API Rilpivirine.[42]

To further corroborate the synthetic utility of our methodology, we decided to perform the widely representative Mizoroki–Heck reaction with substrate **2m**, integrating continuous flow technology with MW irradiation.

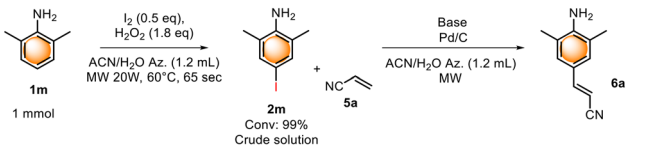

Scheme 3 3-(4-Amino-3,5-dimethylphenyl)-2-propenenitrile (**6a**) synthesis under batch conditions using MW as the heating source.

Table 3 Optimization of the Mizoroki–Heck reaction in batch conditions under MW irradiation

Entry	Base	W	Pd (mol%)	V (mL)	T (°C)	Reaction time (min)	C^a (%)
1	NaOAc	300	0.6	1.2	130	30	10
2	NaOAc	300	0.6	1.2	130	60	24
3	NaOAc	300	1.1	1.2	130	120	51
4	TEA	300	1.1	1.2	130	120	64
5	TEA	300	1.1	1.2	130	180	99

[a] Reaction conditions: 4-iodo-2,6-dimethylaniline (**2m**, 1 mmol) from crude solution, acrylonitrile (**5a**, 1.5 eq.), base (1.2 eq.), ACN/H_2O (84 : 16), 300 W dynamic program, 130 °C. C = conversion to **6a** determined by GLC, and the remaining material is unreacted **2m**.

Table 4 Reaction optimization for the Mizoroki–Heck reaction in continuous flow with MW irradiation for the synthesis of Rilpivirine key intermediate **6a**

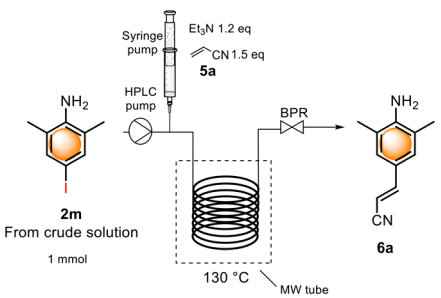

Entry	W	Pd/C (wt/wt)	BPR (psi)	Flow rate (mL min^{-1})	Residence time (min)	C^a (%)
1	300	10%[b]	5	1	—	—
2	150	10%[b]	5	1	—	—
3	150	1%[b]	45	1	—	—
4	70	1%[c]	75	1	5.2	60
5	70	1%[c]	75	0.5	11	99

[a] Reaction conditions: 4-iodo-2,6-dimethylaniline (**2m**, 1 mmol) from crude solution, acrylonitrile (**5a**, 1.5 eq.), TEA (1.2 eq.), ACN/H_2O (84 : 16). Reactor length 1.8 m, C = conversion to **6a** determined by GLC, and the remaining material is unreacted **2m**. [b] Reactor tube size 1/8″ (1/16″ ID) packed with commercially available Pd/C dispersed in quartz powder. [c] Reactor tube size 1/4″ (1/8″ ID) packed with commercially available Pd/C dispersed in 1 mm glass beads.

The Mizoroki–Heck reaction required preliminary optimisation under batch conditions using MW before we could further enhance the system with a modular approach in continuous flow. This optimisation step was accomplished using the crude solution obtained after the iodination reaction, maintaining the ACN/H_2O az as the medium. Our goal in this optimisation step was to achieve 3-(4-amino-3,5-dimethylphenyl)-2-propenenitrile (**6a**), a key intermediate for Rilpivirine synthesis (Scheme 2), from iodination product **2m** and acrylonitrile (**5a**) in the presence of a Pd/C catalyst. After conducting a MW-assisted batch iodination reaction of 2,6-dimethylaniline (**1m**) (Scheme 3), acrylonitrile (**5a**) and the base were added. Following the addition of the appropriate catalytic amount of commercially available Pd/C (10 wt% Pd), the resulting reaction mixture was allowed to react until completion using a dynamic heating method.

Using sodium acetate as a base, we observed that it caused the breakdown of the azeotrope and phase separation, resulting in poor conversions. Increasing the amount of Pd/C and prolonging the reaction time did not change the outcome, which never exceeded 51% conversion over a total of 2 h (Table 3, entry 3). Conversely, switching the base to triethylamine (TEA) markedly improved the conversion (Table 3, entry 4), achieving complete conversion within 180 min without separation of the ACN/H_2O mixture (entry 5).

Pd/C has been selected as representing the benchmark heterogeneous catalyst in many cross-coupling reactions. In addition, previous studies using TEM, XRD, and periodic leaching measurements,[43,44] or *in operando* X-ray[45] analysis, have further confirmed its excellent recoverability features.

At that stage, we attempted to telescope the two processes in a modular MW-assisted flow process, combining the selective iodination reaction with the cross-coupling reaction to obtain the key intermediate of Rilpivirine (**6a**). The reaction mixture derived from the iodination protocol, collected into a reservoir and allowed to cool down to 30 °C, was pumped through a tee section, where it was combined with a premixed solution of neat TEA and acrylonitrile. The resulting solution was directly passed through a reactor packed with commercially available Pd/C (10 wt% Pd) dispersed in various materials (described below), coiled up and placed inside a MW oven equipped with an open vessel attachment (see the SI for further details).

By maintaining the same operating temperature (130 °C), we tried different reaction conditions (Table 4). By decreasing the electrical power of the MW (from 300 to 70 W), we noticed

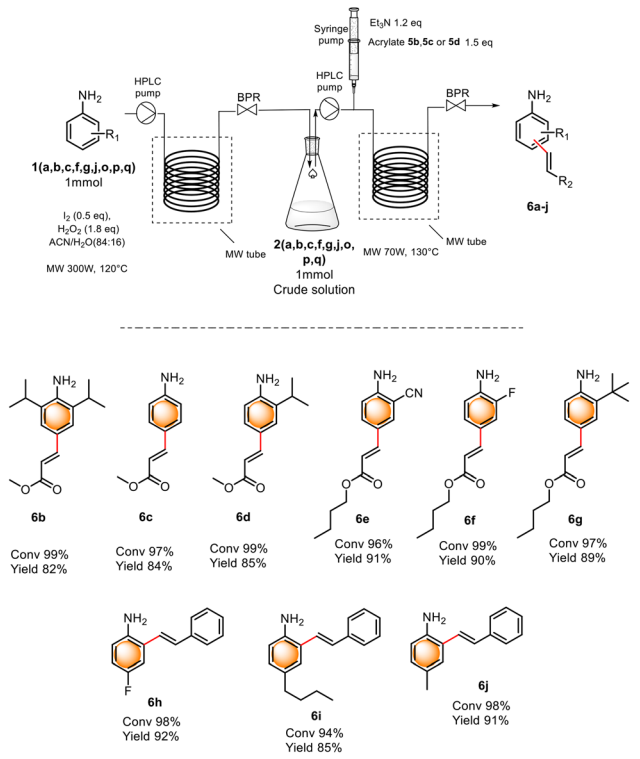

Scheme 4 Substrate scope for a consecutive Mizoroki–Heck reaction in continuous flow with MW irradiation. Reaction conditions: aniline **1** (**a**, **b**, **c**, **f**, **g**, **j**, **o**, **p**, **q**), 1 mmol, I_2 (0.5 eq.), H_2O_2 (1.8 eq.), ACN/H_2O (84 : 16). Fixed power program. 300 W, 120° C, 1 mL min^{-1}. Then, once cooled down to 30 °C, intermediate **2** (**a**, **b**, **c**, **f**, **g**, **j**, **o**, **p**, **q**), acrylate (**5** (**b**, **c**, **d**), 1.5 eq.), TEA (1.2 eq.), ACN/H_2O (84 : 16). Fixed power program. 70 W, 130 °C, 0.5 mL min^{-1}. **5b**: methyl acrylate; **5d**: *n*-butyl acrylate; **5c**: styrene. Yields of the isolated pure products.

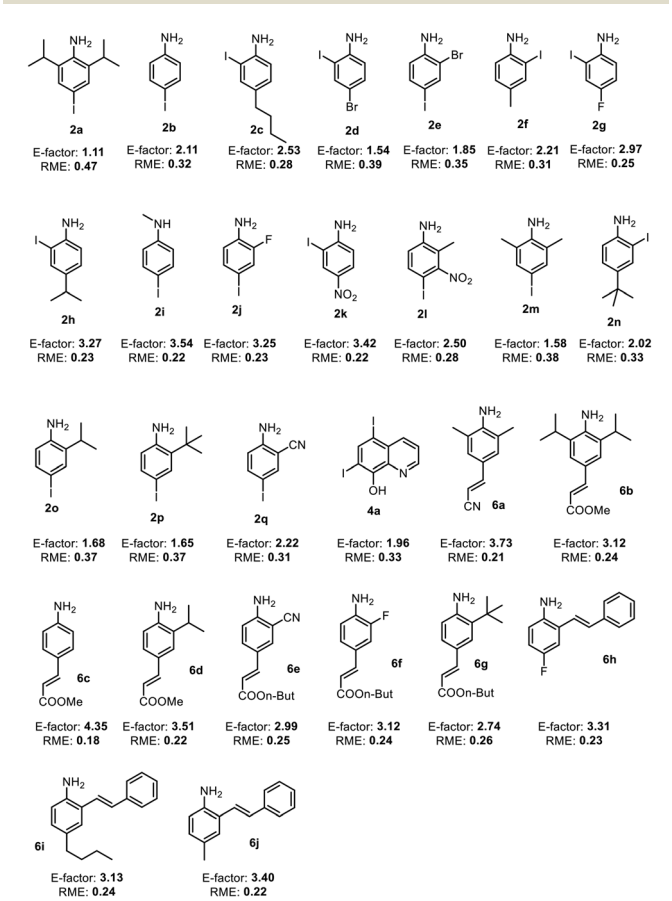

Scheme 5 *E*-Factor and reaction mass efficiency for all synthesized substrates.

Table 5 Comparison of the *E*-factor and RME values

		Compounds					
Ref.		2a	2b	4a	6a	6c	6j
46	*E*-Factor	25.9					
	RME	0.037					
47	*E*-Factor	49.9					
	RME	0.016					
48	*E*-Factor	40.3					
	RME	0.024					
13	*E*-Factor		128.4				
	RME		0.007				
49	*E*-Factor		134.1				
	RME		0.007				
50	*E*-Factor		206.3				
	RME		0.005				
51	*E*-Factor			5.8			
	RME			0.14			
52	*E*-Factor			495.3			
	RME			0.002			
53	*E*-Factor			435.3			
	RME			0.002			
54	*E*-Factor				2.8		
	RME				0.26		
55	*E*-Factor				500.1		
	RME				0.002		
56	*E*-Factor					584.5	
	RME					0.001	
57	*E*-Factor					260.1	
	RME					0.004	
58	*E*-Factor						352.2
	RME						0.003
59	*E*-Factor						84.4
	RME						0.012
This work	***E*-Factor**	**1.11**	**2.11**	**1.96**	**3.73**	**4.35**	**3.40**
	RME	**0.47**	**0.32**	**0.33**	**0.21**	**0.18**	**0.22**

better control over the internal pressure, which was further managed by the BPR to prevent reaction runaway. Indeed, the rapid increase in internal pressure led to unsuccessful trials and reactor breakage. To prevent these issues, we also reduced the mass percentage of Pd/C over the total mass of the reactor filling materials (Table 4, entries 1–3).

Using 1 mm glass beads to disperse the Pd/C catalyst, we achieved 60% conversion to product **6a** (entry 4), and by decreasing the flow rate to 0.5 mL min^{-1}, we smoothly obtained full conversion (entry 5). Subsequent isolation and NMR spectroscopy of the reaction product revealed that **6a** was present in a 70 : 30 *E*/*Z* ratio.

Positively impressed by the exceptional performance of our modular reactor, we tested its robustness and tolerability towards various substrates. In doing so, we synthesized additional substrates using different acrylates and substituted anilines (Scheme 4). In all cases, the final yield of the products was excellent.

Finally, to quantify our efforts regarding process sustainability, we calculated the *E*-factor and RME for all synthesised substrates (Scheme 5) in the iodination step and during the combined iodination and Mizoroki–Heck cross-coupling step (see SI for detailed calculations). By comparing the obtained metrics with the process metrics present in the literature,[46–59] for selected structures (**2a**, **2b**, **4a**, **6a**, **6c**, **6j**) (Table 5) we deduced that, in addition to the obvious advantage of recovering and reusing the azeotropic mixture employed as the reaction medium, there was an intrinsic benefit in using the combined MW-flow system. This system could provide products selectively (for both processes) and with excellent yields, thus eliminating the need for laborious work-up procedures. It is worth noting that the small total volume of the telescoped flow reactor (26 mL) aligns well with the numbering-up strategy to improve scalability and overcome laboratory-scale productivity.

Conclusions

We optimized the conditions for the selective preparation of iodinated anilines by combining MW irradiation with continuous-flow technology. Eighteen substrates were selectively iodinated. We also demonstrated the synthetic utility of our approach by applying it to an approved API (iodoquinol). The utility of iodinated aromatics is widely exemplified by their consequent use in functionalization steps such as the cross-coupling reactions and related transformations. Therefore, we focused on the widely representative Mizoroki–Heck cross-coupling and continuous flow. Starting from a simple aniline, we telescoped iodination and cross-coupling, accessing several

products, including the API Rilpivirine intermediate. As shown by the green metric calculations, combining these two technologies improved the overall sustainability of the process. MW irradiation was used to improve energy efficiency and reduce reaction time while overcoming the scale-up limitations inherent in continuous-flow protocols. We also aimed to minimize waste by employing a reaction medium that could be recovered and recycled almost completely.

Abbreviations

MW	Microwave
RME	Reaction mass efficiency
BPR	Back pressure regulator
PTFE	Polytetrafluoroethylene
API	Active pharmaceutical ingredients
GLC	Gas–liquid chromatography
ACN	Acetonitrile
GVL	γ-Valerolactone
2Me-THF	2-Methyltetrahydrofuran
CPME	Cyclopenthylmethylether
AcOH	Acetic acid
PTSA	*p*-Toluenesulfonic acid
PS-PTSA	Polymer-supported-*p*-toluenesulfonic acid
NaOAc	Sodium acetate
TEA	Triethylamine
Pd/C	Palladium on carbon

Author contributions

The manuscript was written through the contributions of all authors. All authors have given approval to the final version of the manuscript. F. B. and M. B.: investigation, methodology, data analyses, and manuscript preparation and review. F. F.: investigation and manuscript editing. L. L. and F. U.: manuscript editing and review. L. V.: conceptualization, project administration, and manuscript preparation (review and editing).

Conflicts of interest

There are no conflicts of interest to declare.

Data availability

The data supporting the conclusions reached from our study have been included as part of the supplementary information (SI). Supplementary information: general procedures, full characterization of the synthesized compounds, and copies of ^{1}H, ^{13}C and ^{19}F NMR spectra. See DOI: https://doi.org/10.1039/d5gc06815k.

Acknowledgements

This work was supported by the funding from European Union (NextGenerationEU) under the Italian Ministry of University and Research (MUR) National Innovation Ecosystem grant (ECS00000041 – VITALITY). We also thank the University of Perugia and MUR for financial support within the PRIN-2022 project "20223ARWAY – REWIND". F. B. and L. V. thank INPS and SienabioACTIVE s.r.l. for the doctoral grant and training offered to F. B.

References

1 A. Domokos, B. Nagy, B. Szilágyi, G. Marosi and Z. K. Nagy, *Org. Process Res. Dev.*, 2021, **25**, 721–739.
2 S. V. Ley, Y. Chen, A. Robinson, B. Otter, E. Godineau and C. Battilocchio, *Org. Process Res. Dev.*, 2021, **25**, 713–720.
3 (*a*) J. Wegner, S. Ceylan and A. Kirschning, *Adv. Synth. Catal.*, 2012, **354**, 17–577; (*b*) J. Britton and C. L. Raston, *Chem. Soc. Rev.*, 2017, **46**, 1250–1271.
4 L. Capaldo, Z. Wen and T. Noël, *Chem. Sci.*, 2023, **14**, 4230–4247.
5 D. Alberico, M. E. Scott and M. Lautens, *Chem. Rev.*, 2007, **107**, 174–238.
6 Z. Huang and G. Dong, *Acc. Chem. Res.*, 2017, **50**, 465–471.
7 M. B. Plutschack, B. Pieber, K. Gilmore and P. H. Seeberger, *Chem. Rev.*, 2017, **117**, 11796–11893.
8 V. Hessel, S. Mukherjee, S. Mitra, A. Goswami, N. N. Tran, F. Ferlin, L. Vaccaro, F. M. Galogahi, N. Nguyen and M. Escaribá-Gelonch, *Green Chem.*, 2024, **26**, 9503–9528.
9 S. Santoro, F. Ferlin, L. Ackermann and L. Vaccaro, *Chem. Soc. Rev.*, 2019, **48**, 2767–2782.
10 J. Park, S. H. Kim and J. Cho, *Green Chem.*, 2025, **27**, 3284.
11 D. Cantillo and C. O. Kappe, *React. Chem. Eng.*, 2017, **2**, 7–19.
12 B. Li and Y. Hu, *Chem. – Eur. J.*, 2023, **29**, e202301336.
13 N. Mali, J. G. Ibarra-Gutiérrez, L. I. Lugo Fuentes, R. Ortíz-Alvarado, L. Chacón-García and P. Navarro-Santos, *Eur. J. Org. Chem.*, 2022, e202201067.
14 P. Bovonsombat, W. Lorpaiboon, S. Laoboonchai, P. Sriprachaya-anunt, W. Yimkosol and N. Siriphatcharachaikul, *Tetrahedron Lett.*, 2020, **61**, 152461.
15 S. N. Joshi, S. M. Vyas, H. Wu, M. W. Duffel, S. Parkin and H. J. Lehmler, *Tetrahedron*, 2011, **67**, 7461–7469.
16 (*a*) P. L. Anelli, M. Brocchetta, L. Lattuada and F. Uggeri, *Pure Appl. Chem.*, 2011, **84**, 485–491; (*b*) H. J. M. Gijsen, H. C. C. K. Van Bakel, W. Zwaan and L. A. Hulshof, *Org. Process Res. Dev.*, 1999, **3**, 38–43.
17 (*a*) J. L. Osorio-Tejada, F. Ferlin, L. Vaccaro and V. Hessel, *Green Chem.*, 2023, **25**, 9760–9778; (*b*) M. Breugst and D. von der Heiden, *Chem. – Eur. J.*, 2018, **24**, 9187–9193.
18 A. K. Banerjee, W. Vera, H. Mora, M. S. Laya, L. Bedoya and E. V. Cabrera, *J. Sci. Ind. Res.*, 2006, **65**, 299–308.

19 C. Monnereau, E. Blart and F. Odobel, *Tetrahedron Lett.*, 2005, **46**, 5421–5423.
20 A. Sutherland and N. Sloan, *Synthesis*, 2016, 2969–2980.
21 P. M. Jadhav, A. B. Rode, L. Kótai, R. P. Pawar and S. U. Tekale, *New J. Chem.*, 2021, **45**, 16389–16425.
22 F. Valentini, B. Di Erasmo, M. Ciani, S. Chen, Y. Gu and L. Vaccaro, *Green Chem.*, 2024, **26**, 4871.
23 (*a*) E. Petricci, C. Risi, F. Ferlin, D. Lanari and L. Vaccaro, *Sci. Rep.*, 2018, **8**, 10571; (*b*) K. Martina, G. Cravotto and R. S. Varma, *J. Org. Chem.*, 2021, **86**, 13857–13872.
24 T. N. Glasnov and C. O. Kappe, *Chem. – Eur. J.*, 2011, **17**, 11956–11968.
25 A. Diaz-Ortiz, P. Prieto and A. de la Hoz, *Chem. Rec.*, 2019, **19**, 85–97.
26 S. B. V. Junne, Y. Vibhute and V. M. Gurav, *Int. J. ChemTech Res.*, 2009, **1**, 1005–1007.
27 M. Sosnowski, L. Skulski and K. Wolowik, *Molecules*, 2004, **9**, 617–621.
28 C. Kuzemko, M. Blondeel, M. Bradshaw, G. Bridge, E. Faigen and L. Fletcher, *Geopolitics*, 2024, **30**, 531–565.
29 F. Ferlin, P. M. Luque Navarro, Y. Gu, D. Lanari and L. Vaccaro, *Green Chem.*, 2020, **22**, 397–403.
30 S. Karim, H. M. Saw and Y. Ting, *Green Chem.*, 2024, **26**, 4112–4126.
31 F. Ferlin, F. Valentini, F. Campana and L. Vaccaro, *Green Chem.*, 2024, **26**, 6625–6633.
32 M. U. Luecher and F. Gallou, *Green Chem.*, 2024, **26**, 5239–5252.
33 E. Lucas, A. J. Martin and S. Mitchell, *Green Chem.*, 2024, **26**, 9300–9309.
34 A. Bardow, J. Perez-Ramirez, S. Sala and L. Vaccaro, *Green Chem.*, 2024, **26**, 11016–11018.
35 D. Crespi, *Green Chem.*, 2025, **27**, 12107–12114.
36 (*a*) F. Campana, D. Lanari, F. De Angelis and L. Vaccaro, *Green Chem.*, 2025, **27**, 11903–11913.
37 F. Valentini and L. Vaccaro, *Molecules*, 2020, **25**, 5264.
38 (*a*) F. Ferlin, F. Valentini, D. Sciosci, M. Calamante, E. Petricci and L. Vaccaro, *ACS Sustainable Chem. Eng.*, 2021, **9**, 12196–12204; (*b*) G. Quaglia, F. Campana, L. Latterini and L. Vaccaro, *ACS Sustainable Chem. Eng.*, 2022, **10**, 9123–9130.
39 (*a*) F. Valentini, F. Ferlin, E. Tomarelli, H. Mahmoudi, M. Bagherzadeh and M. Calamante, *ChemSusChem*, 2021, **14**, 3359–3366; (*b*) S. Trastulli Colangeli, F. Campana, F. Ferlin and L. Vaccaro, *Green Chem.*, 2024, **27**, 633–641.
40 (*a*) F. Ferlin, V. Trombettoni, L. Luciani, S. Fusi, O. Piermatti, S. Santor and L. Vaccaro, *Green Chem.*, 2018, **20**, 1634–1639; (*b*) F. Campana, D. Lanari, A. Marrocchi and L. Vaccaro, Green solvents for organic electronics processing, in *Sustainable Strategies in Organic Electronics*, Elsevier, Amsterdam, 2022, ch. 12, pp. 426–445.
41 (*a*) *The Merck Index*, 15th edn, 2013, p. 937; (*b*) R. W. Huigens III, Y. Abouelhassan and A. Garrison, *Combination therapy for treating infectious diseases*, University of Florida Research Foundation, INC., US, 2016.
42 (*a*) K. Delacroix, B. Fours, S. Kowalkowski, V. Revil-Baudard, M. Perez and L. Petit, *Org. Process Res. Dev.*, 2024, **28**, 524–531; (*b*) D. P. R. W. Schils, B. P. A. M. J. Medaer, E. T. J. Pasquier, P. A. J. Janssen, J. Heeres and R. G. G. Leenders, *Processes for the preparation of 4-[[4-[[4-(2-cyanoethenyl)-2,6-dimethylphenyl]amino]-2-pyrimidinyl]amino]benzonitrile*, Plasseraud id, FR, 2002.
43 B. Di Erasmo, E. Bazzica, G. Brufani, C. Li and L. Vaccaro, *ACS Sustainable Chem. Eng.*, 2025, **13**, 12220–12231.
44 G. Brufani, S. Chen, M. T. Tiberi, F. Campana, E. Paone, Y. Gu, F. Mauriello and L. Vaccaro, *Green Chem.*, 2025, **27**, 3869–3878.
45 M. A. Newton, J. B. Brazier, E. M. Barreiro, S. Parry, H. Emmerich, L. A. Adrio, C. J. Mulligan, K. Hellgardt and K. K. Hii, *Green Chem.*, 2016, **18**, 406–411.
46 H. Yang, G. Li, Z. Ma, J. Chao and Z. Guo, *J. Catal.*, 2010, **276**, 123–133.
47 M. Zhang, Z. Xu and D. Shi, *Tetrahedron*, 2021, **79**, 131861.
48 G. A. Price, A. R. Bogdan, A. L. Aguirre, T. Iwai, S. W. Djuric and M. G. Organ, *Catal. Sci. Technol.*, 2016, **6**, 4733–4742.
49 R. M. Appa, B. Ramesh Naidu, D. Venkateswarl, M. M. Hanafiah, S. K. Lakkaboyana and J. Lakshmidevi, *Green Chem. Lett. Rev.*, 2021, **14**, 700–712.
50 D. W. Slocum, K. C. Tekin, Q. Nguyen, P. E. Whitley, T. K. Reinscheld and B. Fouzia, *Tetrahedron Lett.*, 2011, **52**, 7141–7145.
51 S. Thangalipalli, S. Goud Bandalla and C. Kiran Neella, *ChemistrySelect*, 2023, **8**, e202204338.
52 L. Lista, A. Pezzella, A. Napolitano and M. d'Ischia, *Tetrahedron*, 2008, **64**, 234–239.
53 A. Deshmukh, B. Gore, H. V. Thulasiram and V. P. Swamy, *RSC Adv.*, 2015, **5**, 88311–88315.
54 B. H. Lipshutz, N. A. Isley, J. C. Fennewald and E. D. Slack, *Angew. Chem., Int. Ed.*, 2013, **52**, 10952–10958.
55 S. Sergeyev, A. K. Yadav, P. Franck, J. Michiels, P. Lewi and J. Heeres, *J. Med. Chem.*, 2016, **59**, 1854–1868.
56 A. Mohammadinezhad and B. Akhlaghinia, *Green Chem.*, 2017, **19**, 5625–5634.
57 F. Ortega-Jiménez, F. X. Domínguez-Villa, A. Rosas-Sánchez, G. Penieres-Carrillo, J. G. López-Cortés and M. C. Ortega-Alfaro, *Appl. Organomet. Chem.*, 2015, **29**, 556–560.
58 T. Drennhaus, D. Leifert, J. Lammert, J. P. Drennhaus, K. Bergander and C. G. Daniliuc, *J. Am. Chem. Soc.*, 2023, **145**, 8665–8676.
59 T. Mandal, S. Mallick, N. Kumari and S. De Sarkar, *Org. Lett.*, 2022, **24**, 8452–8457.